**AUTHOR QUERY FORM**

Dear Author,

Please check your proof carefully and mark all corrections at the appropriate place in the proof (e.g., by using on-screen annotation in the PDF file) or compile them in a separate list. Note: if you opt to annotate the file with software other than Adobe Reader then please also highlight the appropriate place in the PDF file. To ensure fast publication of your paper please return your corrections within 48 hours.

For correction or revision of any artwork, please consult http://www.elsevier.com/artworkinstructions.

Any queries or remarks that have arisen during the processing of your manuscript are listed below and highlighted by flags in the proof. Click on the 'Q' link to go to the location in the proof.

| Location in article | Query / Remark: **click on the Q link to go** <br> **Please insert your reply or correction at the corresponding line in the proof** |
|---|---|
| Q1 | Please confirm that given names and surnames have been identified correctly. ← Ok. |
| Q2 | The citation "Vehí et al., 2001" has been changed to match the author name/date in the list. Please check here and in subsequent occurrences, and correct if necessary. ← Thanks |
| Q3 | Highlights ... spaces. H... were not c... more infor... <br> - An aridification trend is observed in the Mediterranean area in the Late Pliocene <br> - Climate and vegetation cyclical changes (glacial-interglacial variability) occurred <br> - Climate changes in the Mediterranean area were mostly forced by precession |
| Q4, Q6 | The citation "Kloosterboer-van Hoeve, 2006" has been changed to match the ... name/date in the reference list. Please check here and in subsequent occurrences, and correct if necessary. ← Ok |
| Q5 | Citation "Burjachs, 1990" ha... details for this reference. Ok, it has been changed for Burjachs et al.. 2003 |
| Q7 | Uncited references: This section comprises references that occur in the reference list but not in the body of the text. Please position each reference i... ← Ok. ...delete it. Thank you. |
| Q8 | Please verify if appropriate that Figure Appendix 3 is captured as part of the proof since this was originally labeled as "Supp. Fig. 3" in the source manuscript. ← Ok, thanks |
| | Please check this box if you have no corrections to make to the PDF file. ☐ |

Thank you for your assistance.

# Late Pliocene vegetation and orbital-scale climate changes from the western Mediterranean area

Gonzalo Jiménez-Moreno [a,*], Francesc Burjachs [b,c,d], Isabel Expósito [c,d], Oriol Oms [e], Ángel Carrancho [f,g], Juan José Villalaín [f], Jordi Agustí [b,c,d], Gerard Campeny [c,d], Bruno Gómez de Soler [c,d], Jan van der Made [h]

[a] Departamento de Estratigrafía y Paleontología, Universidad de Granada, Spain
[b] ICREA, Barcelona, Spain
[c] IPHES, Tarragona, Spain
[d] Universitat Rovira i Virgili, Tarragona, Spain
[e] Universitat Autònoma de Barcelona, Spain
[f] Departamento de Física, Universidad de Burgos, Spain
[g] CENIEH, Burgos, Spain
[h] Museo Nacional de Ciencias Naturales, CSIC, Madrid, Spain

**A B S T R A C T**

The Late Pliocene is a very interesting period as climate deteriorated from a warm optimum at ca. 3.3–3.0 Ma to a progressive climate cooling. Simultaneously, the Mediterranean area witnessed the establishment of the Mediterranean-type seasonal precipitation rhythm (summer drought). These important climate changes produced significant vegetation changes, such as the extinction of several thermophilous and hygrophilous plant taxa from the European latitudes. Besides these long-term trends, climate was also characterized by cyclical variability (i.e., orbital changes) that forced vegetation changes (forested vs. open vegetation). In the Mediterranean area, cyclical changes in the vegetation were mostly forced by precession. In this study we analyzed pollen from a Late Pliocene maar lake core from NE Spain. An increase in aridity is observed as well as cyclic variations throughout the studied sequence. Cyclicity was mostly forced by precession but also by obliquity and eccentricity. Precipitation seems to be the main factor controlling these cycles. These data allowed estimating a sedimentary rate of ca. 0.19 mm/yr and the time duration covered by the studied core, close to 200 ka. The combination of biostratigraphy, palaeomagnetism and cyclostratigraphy allowed for a very precise dating of the sediments between ca. 3.3 and 3.1 Ma. Climate and paleobiogeographical implications are discussed within the context of the Late Pliocene Northern Hemisphere glacial intensification.

© 2013 Published by Elsevier B.V.

## 1. Introduction

The Late Pliocene (Piazencian stage; ca. 3.6–2.6 Ma) is a very interesting period. Around 3.3–3.0 Ma, during the Pliocene thermal maximum, temperatures were similar to those projected for the end of this century, about 2°–3 °C warmer globally on average than today (IPCC, 2007). Therefore, this period has been studied in detail as it is thought to be a very good analog for future climate change (Robinson et al., 2008). Later on progressive colder conditions related with an intensification of Northern Hemisphere glaciations occurred (Zachos et al., 2001). A progressive aridification in the Mediterranean area also happened at this time (Suc, 1984; Leroy and Dupont, 1994; Fauquette et al., 1998; Khélifi et al., 2009; Popescu et al., 2010) as well as the establishment of the Mediterranean-type seasonal precipitation rhythm (summer drought at 3.4 Ma; Suc, 1984; Suc and Popescu, 2005; Barrón et al., 2010; Jiménez-Moreno et al., 2010). These changes dramatically affected past terrestrial environments in the Mediterranean area and vegetation experienced a decrease and the disappearance of many thermophilous and hygrophilous species and the increase in xerophytes and Mediterranean adapted taxa (Suc, 1984; Popescu et al., 2010).

Besides these long-term trends, climate during the Late Pliocene was also characterized by cyclical variability (i.e., orbital changes) that forced vegetation changes (forested vs. open vegetation; Tzedakis, 2007; Popescu et al., 2010). In the Mediterranean area, cyclical changes in the vegetation are mostly forced by precession (Kloosterboer-van Hoeve et al., 2006; Tzedakis, 2007; Sánchez Goñi et al., 2008). Nevertheless, obliquity also played an important role in shaping the vegetation during the 2.8–1.0 Ma period (Joannin et al., 2007, 2008; Popescu et al., 2010; Suc et al., 2010). However, there is a lack of these kinds of studies in this area and the long-term vegetation changes are only documented in a few palynological studies on marine sediments (Suc, 1984; Bertini, 2001; Combourieu Nebout et al., 2004; Jiménez-Moreno et al., 2010). Therefore, high-resolution pollen studies are needed to improve our knowledge about the main forcing triggering millennial-scale vegetation changes during the Late Pliocene in the Mediterranean area.

\* Corresponding author. Tel.: +34 958 248727.
E-mail address: gonzaloj@ugr.es (G. Jiménez-Moreno).

In this study we present a high-resolution palynological analysis, paleomagnetic and magnetic susceptibility data from a sediment core from a maar lake in NE Spain, which provides a continuous record of paleoenvironmental variations in the western Mediterranean area during the Late Pliocene. The pollen data have been compared with the available magnetic susceptibility and lithological changes. These data demonstrate cyclic and paired changes in vegetation, lake level and sedimentation that appear to be linked to orbital-scale climate variability (i.e., "glacial–interglacial" cycles). Climate, paleobiogeographical and age implications are discussed within the context of the Late Pliocene Northern Hemisphere glacial intensification.

### 1.1. Maar lakes

A maar is a low-relief broad crater formed after an explosive phreatomagmatic eruption. These craters rapidly filled up with ground water and form a lake. Sedimentary records from maars have been proven to be very good records for paleoecological studies (Pirrung et al., 2003). Maars are usually deep, characterized by anoxic bottom conditions and laminated sedimentation. They are also ground water fed, less subject to surface runoff and evaporation, and thus sedimentation is continuous (i.e., Willis et al., 1999; Pirrung et al., 2003; Lenz et al., 2010). In addition, maars are endorheic basins, subject to very similar and internal processes for comparison.

Sedimentation in these basins is usually very constant until the lake gets filled up with sediment. The typical evolution of the sedimentary sequences is the following: syn/post-eruptive wall rock debris and pyroclastic breccias characterize the bottom deposits and are followed by a fining-upward sequence of lacustrine muds and final shallow lake-marsh deposits (see Pirrung et al., 2003 and references therein). Because of the same shape and internal dynamics, sedimentary rates oscillate between 0.14 and 0.82 mm/yr (Negendank et al., 1982; Watts, 1985; Willis et al., 1999; Leroy et al., 2000; Galán et al., 2009; Lenz et al., 2010).

Maar lakes are generally meromictic, so their anoxic bottom waters are a potential place for fossil preservation (see references in Gómez de Soler et al., 2012). In the case of pollen analysis, the mudstone lacustrine part of maar successions is of particular interest.

### 1.2. Camp dels Ninots

The Camp dels Ninots maar (41° 50′ 06″N, 2° 47′ 51″E; 95 m above sea level) is located in Caldes de Malavella, Girona, NE Spain (Fig. 1). Mean annual temperature in this area (Girona) is ca. 14 °C. Mean annual precipitation is around 730 mm. This maar was elliptical in shape with a diameter between 650 and 400 m. It formed after phreatovolcanism affected the Paleozoic bedrock during a Pliocene distensive tectonic phase in this area (Gómez de Soler et al., 2012) and is part of the Catalan Volcanic Complex, which occurred between 14 Ma and 10 ka in NE Spain (Gómez de Soler et al., 2012). Volcanism in this area was alkaline with olivine-rich basaltic flows and volcanic cones with both explosive and non-explosive activity phases (see references in Gómez de Soler et al., 2012). Volcanic rocks, including basalt flows, occur around the studied basin (Gómez de Soler et al., 2012).

The Camp dels Ninots volcano was first identified by Vehí et al. (1999) who described the stratified deposits as lake sediments filling the crater. Mammal bones were also found in the maar lake sediments and several excavations have been carried out since 2003 in the area (Gómez de Soler et al., 2012). At present, ten large mammal skeletons in anatomical connection have been recovered, including six bovids (Alephis tigneresi), a rhino (Stephanorhinus jeanvireti) and three tapirs (Tapirus arvernensis), as well as turtles (Mauremys leprosa), amphibians (cf. Pleurodeles sp., Lissotriton aff. helveticus and Pelophylax cf. perezi), freshwater fish (Leuciscus?) and a rodent (Apodemus atavus), some of them in anatomical connection. The excellent fossil preservation makes this site a Konservat-Lagerstätte (Gómez de Soler et al., 2012).

The sedimentary infill of the Camp dels Ninots maar has been characterized during the different excavations and through two drillings that were carried out in the basin in 2009. The basin infill is characterized by the typical vertical stratigraphic succession in maars (Pirrung et al., 2003; Lindner et al., 2006; among others). Syn-/post-eruptive wall rock debris and pyroclastic breccias characterize the bottom
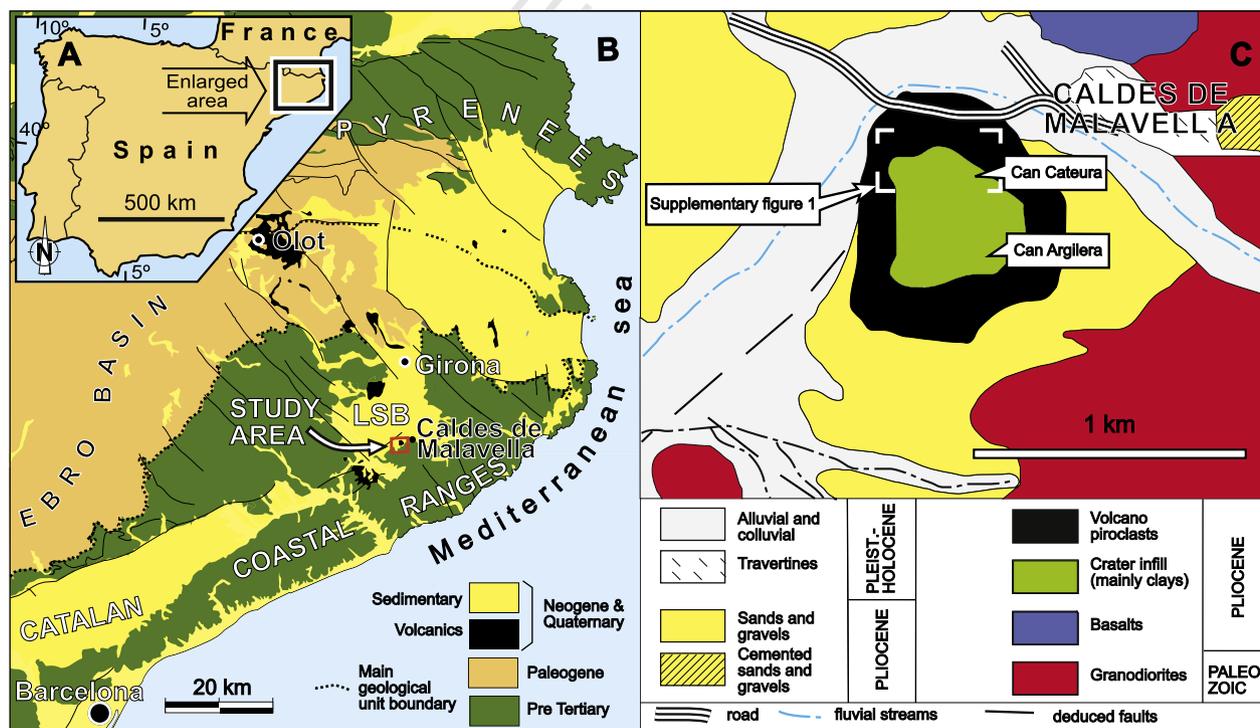


Fig. 1. Geological map of the Camp dels Ninots Volcano. A and B) Location within the main geological units from NE Iberia. LSB: La Selva Basin. C) Detailed geology from the area and extension of the crater. The location of the CC09 core is shown (Can Cateura).
Q2     Panel C is modified from Vehí (2001).

deposits and are followed by a fining-upwards sequence of lacustrine muds with coarse layers and final shallow lake deposits.

## 2. Materials and methods

Two cores were collected in July 2009 from the Camp dels Ninots basin: a ca. 30 m-long core (Can Argilera core, CA09) from the basin margin and a longer ca. 75 m-long (Can Cateura core, CC09) core from the center of the basin. Coring was carried out using a percussion system, which allowed azimuthal orientation through a continuous line-mark left by the drilling device during the coring process. In this study we analyzed the longer CC09 core, as it features thicker organic-rich lacustrine facies (Fig. 2).

The general lithology description and paleomagnetic sampling from CC09 (Fig. 2) was mainly carried out in the field as the core was being recovered. Paleomagnetic sub-sampling of the upper 46 m of the CC09 core was performed using quadrangular non-magnetic device, collecting 88 oriented specimens with an average sampling interval of ca. 0.5 m. All samples were encapsulated in cubic plastic boxes (8 cm$^3$) and stored in cold conditions (3–4 °C) to avoid chemical alterations. Additionally, 27 oriented specimens were collected in the same way in a subsequent sampling for thermal demagnetization of the natural remanent magnetization (NRM). These latter specimens correspond to the upper 19 m of the CC09 core.

All paleomagnetic and rock-magnetic analyses were carried out at the Laboratory of Paleomagnetism at Burgos University (UBU). The measurement of the NRM was performed with a 2G SQUID magnetometer (noise level $5 \times 10^{-12}$ Am$^2$). Low-field magnetic susceptibility ($\chi$lf) was measured on each specimen with a KLY-4 Kappabridge (noise level $3 \times 10^{-8}$ S.I.). After a previous pilot study on representative samples of each lithology, a systematic stepwise alternating field demagnetization of the NRM (up to 100 mT) was carried out on the entire set of samples. Stepwise thermal demagnetization was carried out on the 27 specimens sub-sampled in the CC09 core up to 400 °C. After

each thermal demagnetization step, the low-field magnetic susceptibility was measured to evaluate mineralogical alterations. Over 350–400°, samples displayed erratic directions due to mineralogical alteration upon heating. In order to further study the magnetic carriers and evaluate the magnetic stability, we carried out several rock-magnetic experiments on representative samples from each litho-stratigraphic unit. With the aim of a Variable Field Translation Balance (MMVFTB) we measured: 1) progressive isothermal remanent magnetization (IRM) acquisition curves; 2) hysteresis loops ($\pm 1$ T); 3) back-field curves and 4) thermomagnetic curves (J vs. T$^a$) up to 700 °C in air.

Samples for pollen analysis (2 cm$^3$) were taken every 10 cm throughout the core. A total of 122 pollen samples were analyzed with an average sampling of ca. 25 cm between samples (Fig. 3). Samples were treated following a modified Goeury and Beaulieu (1979) methodology by Burjachs et al. (2003), including hydrochloric acid (HCl), followed by KOH digestion, concentration using Thoulet heavy liquid, and finally with hydrofluoric acid (HF). Counting was performed at 400× magnification to a minimum pollen sum of 300 terrestrial pollen grains. Spores were counted but were not represented in the pollen diagram due to their low representation. Fossil pollen was identified using published keys (Faegri and Iversen, 1989; Beug, 2004) and a modern pollen reference collection. A summary of important pollen type percentages is plotted in Fig. 3. Percentages were calculated with respect to the total pollen sum not including *Pinus*. The pollen zonation was accomplished by cluster analysis of the pollen percentages using CONISS (Grimm, 1987). *Botryococcus* (Algae) was also found and its percentage was calculated with respect to the non-pollen palynomorph sum (Fig. 3). Microcharcoal particles were also counted and the results were expressed in concentrations (fragments of microcharcoal per 1 g of dry sediment; Loublier, 1978; Burjachs, 1990).

Principal Components Analysis (PCA) using PAST (Hammer et al., 2001) was run on the pollen data. This was done to find hypothetical variables (components; i.e., climate parameters) accounting for as much as possible of the variance in the pollen data. A PCA correlation loading
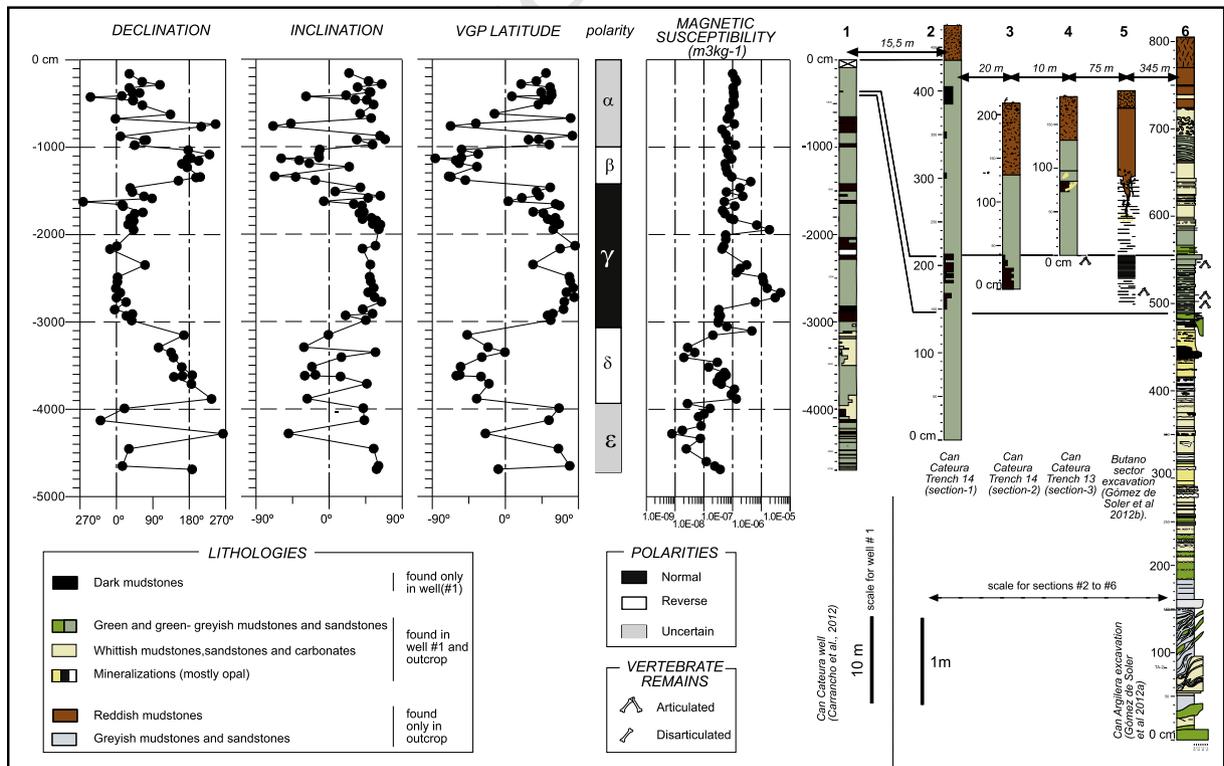


**Fig. 2.** Lithological log of the CC09 core (1; Can Cateura well). Its correlation with the mammal sites discovered in the maar basin (stratigraphic logs 4–6) is shown. See Figure Appendix 1 for more graphic information on how this correlation was done. The characteristic remanence declination, inclination, VGP (Virtual Geomagnetic Pole) latitude and magnetic susceptibility are plotted as a function of depth. The interpreted polarity zones according to the legend are also shown. See Section 4.4 for explanation.

**Fig. 3.** Pollen and charcoal diagram of the Camp dels Ninots CC09 core record showing percentages of selected taxa. *Pinus* was excluded from the total pollen sum due to its very high abundance. The zonation, on the right, was made using cluster analysis provided by CONISS (Grimm, 1987). Gray shading is a 10× exaggeration of the pollen percentages. *Botryococcus* were calculated with respect to the total non-pollen palynomor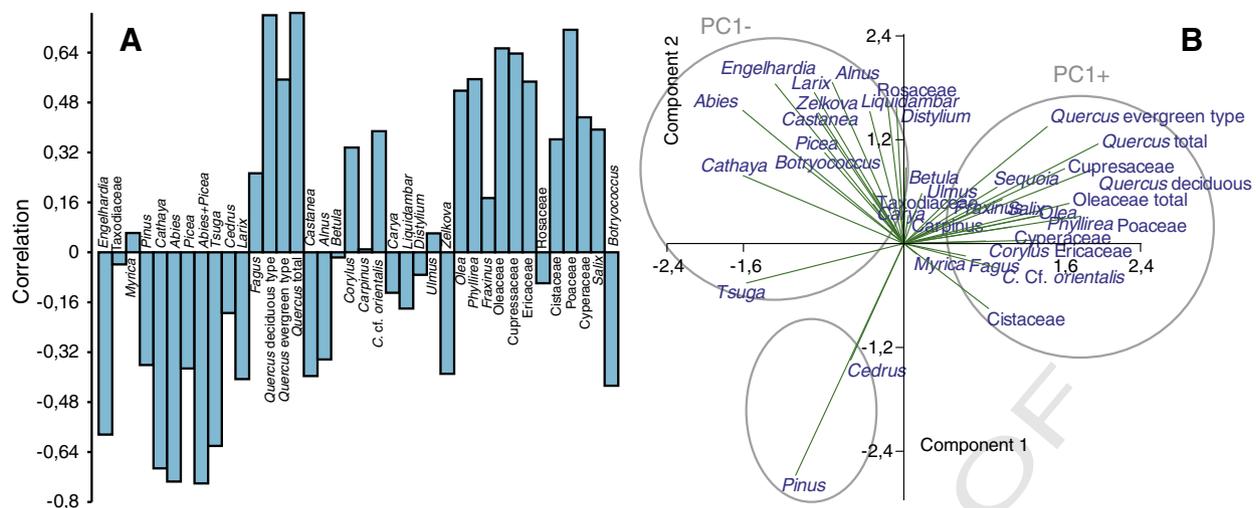ph sum. In green, yellow and blue are percentages the forest, shrubs and herbs and aquatics taxa respectively. Oleaceae include *Olea, Phillyrea* and very rare percentages of *Fraxinus*. The charcoal remains were represented in concentrations (particles per gram of dry sediment, Loublier, 1978). (For interpretation of the references to color in this figure legend, the reader is referred to the web version of this article.)

and scatter diagrams are shown in Fig. 4. These diagrams show to what degree the different taxa correlate with the different components.

A cyclostratigraphic analysis was performed on the most significant raw pollen percentages and MS throughout the studied sequence (Fig. 5). We used the software PAST (Hammer et al., 2001) with the objective of characterizing the different periodicities present in the unevenly spaced raw pollen data and estimating their red-noise spectra. The spectral analysis assisted in identifying recurrent features or periodicities through spectral peaks registered at differing frequencies throughout the studied core.

Filtering the percentage of humid trees at the most important frequency bands was carried out using PAST (Hammer et al., 2001; Fig. 6). Filtering out certain frequency bands in a time series can be useful to smooth a curve, remove slow variation, or emphasize certain periodicities (e.g. Milankovitch cycles).

## 3. Results

### 3.1. Lithology, magnetic susceptibility, paleomagnetism and age control

The CC09 core displays three main sediment types (Fig. 2). (1) The most abundant sediments are laminated green-to-grayish mudstones build up of clay minerals and other clastic grains. These are relatively organic-matter depleted and contain abundant diatoms. (2) Laminated dark mudstones (basically blackish and brownish) are also abundant. These are rich in organic matter and also contain diatoms, clay minerals and other clastic grains. (3) Less abundant are laminated/massive whitish carbonates. Precipitates of opal nodules, together with other diagenetic structures, are mainly concentrated in these later sediments. Dark mudstones (anoxic) are restricted to central parts of the maar basin (sections 1–4 in Fig. 2; Fig. A.1).

Initial natural remanent magnetization (NRM) intensities and magnetic susceptibility values among CC09 samples vary more than two orders of magnitude due to the variation of the concentration of ferromagnetic (*s.l.*) minerals produced by lithological changes. The $NRM_0$ varies between 0.01 and 191 $mAm^{-1}$ while magnetic susceptibility oscillates between $1.78 \times 10^{-9}$ and $4.64 \times 10^{-6}$ $m^3\,kg^{-1}$ (Fig. 2). The magnetic susceptibility variations covary with lithological changes. Thus, lower values are recorded in carbonates. In mudstones, relatively lower and higher values are roughly found in dark and green mudstones, respectively. Despite some values out of range (always in green mudstones), a background trend to higher MS is observed, likely to correlate with the general trend to more clastic conditions towards the top of the core.

In order to assist the paleomagnetic interpretation, different magnetozones have been distinguished depending on the directional behavior observed along the sequence. These are: "Alpha" (top 10 m), "Beta" (between 10 and 15 m depth), "Gamma" (15–30 m depth), "Delta" (30–38 m depth) and "Epsilon" (39–47 m depth). This classification is based on the directional behavior observed and does not keep any relationship with the sedimentological changes distinguished.

Representative alternating field (AF) and thermal demagnetization diagrams (Fig. A.2A–H) show that samples typically contain two magnetization components. After removal of a low-coercivity (<16–18 mT) or low-temperature component (<150–200 °C), the characteristic remanent magnetization (ChRM) direction defines its trajectory linearly towards the origin of orthogonal plots up to 80–100 mT or

**Fig. 4.** Principal Components Analysis (PCA) from the CC09 pollen data. A PCA correlation loading (to Component 1) and scatter diagrams are shown in A and B, respectively. The analysis was carried out using PAST (Hammer et al., 2001). PCA groups are shown.

320–340 °C. The ChRM direction in AF demagnetized specimens from beta and gamma zones is mostly defined up to maximum fields of 35–45 mT due to the presence of spurious gyroremanent magnetizations (GRMs; Fig. A.2D and F). Maximum unblocking temperatures suggest the presence of greigite as the responsible of the GRMs (Fig. A.2B, E and H). A steep increase in the magnetic susceptibility (measured after each demagnetization step at room temperature) indicates that most samples alter the magnetic mineralogy when heated above 330–340 °C. This can be explained by the heating-induced transformation of paramagnetic minerals and/or even greigite.

The ChRM directions were used to calculate virtual geomagnetic pole (VGP) latitudes in order to illustrate the magnetic polarity of the sequence (Fig. 2). In the first 6 m of the alpha zone, several samples with a normal paleomagnetic component were identified. However, it was not possible to reliably determine the magnetic polarity of this interval of the sequence due to the presence of samples with anomalous directions together with other magnetically unstable. Samples corresponding to β and γ magnetozones exhibited stable ChRM components, reasonably intense and of reverse (β) and normal magnetic polarity (γ), respectively (Fig. A.2D–H). Despite most samples from δ zone had demagnetization diagrams of poor quality they defined a reverse ChRM component (Fig. A.2C). The epsilon zone contained few interpretable samples with poorly defined characteristic components showing both normal and reverse polarities but in general of quite unstable magnetization. Because of the anomalous and unstable behavior of these samples it was not possible to determine a reliable polarity here.
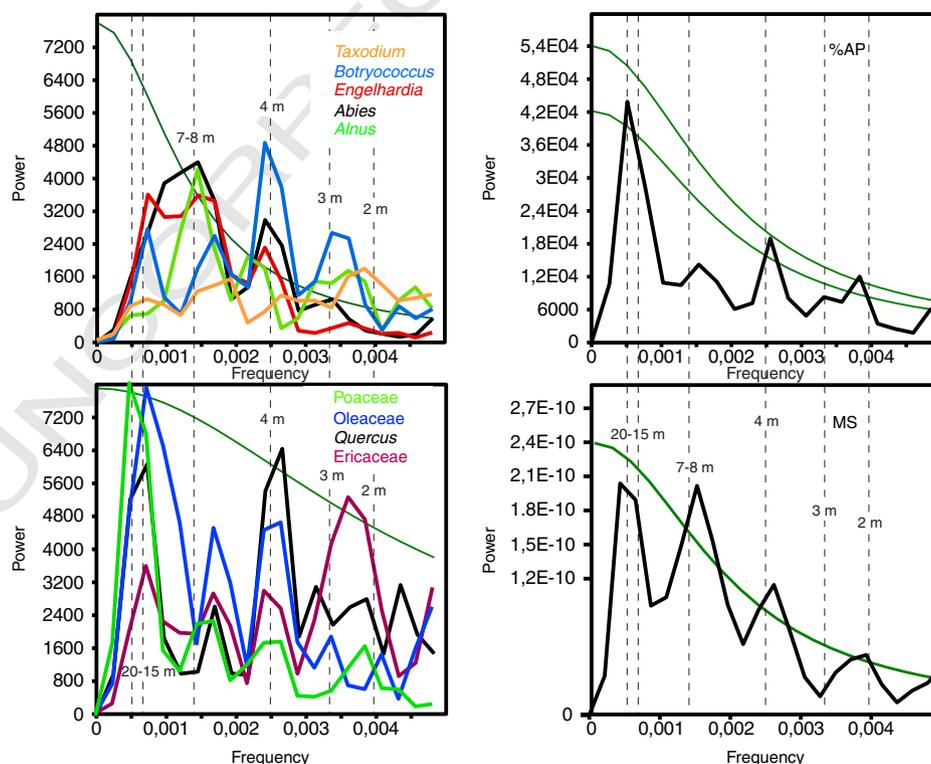


**Fig. 5.** Spectral analysis of the most significant raw pollen taxa and magnetic susceptibility (MS) from the CC09 record. Confidence levels are shown in green. Significant periodicities (above the 80% confidence level) at 2, 3, 4, 7–8 and 15–20 m are highlighted with dashed lines. We used the software PAST (Hammer et al., 2001). (For interpretation of the references to color in this figure legend, the reader is referred to the web version of this article.)
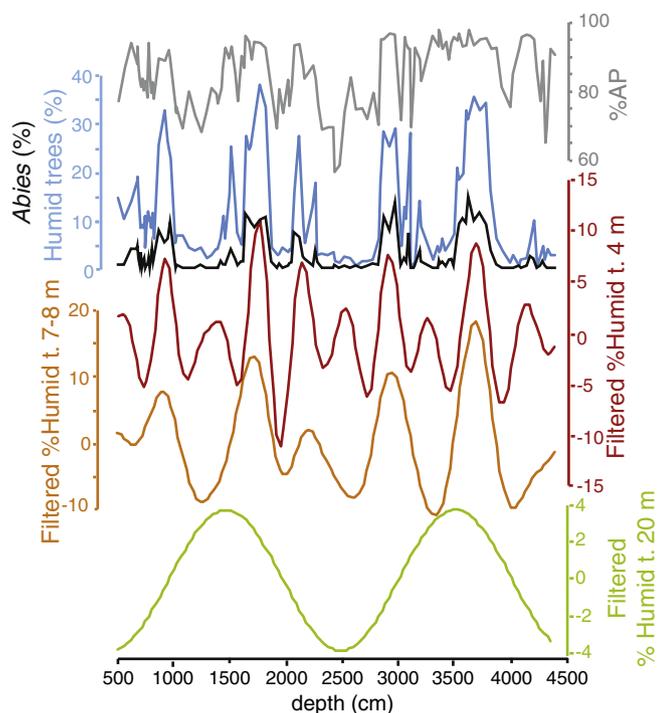
**Fig. 6.** Comparison of filtered 4, 7–8 and 20 m components of the pollen percentage of humid trees (humid t.) with the unfiltered pollen percentages of humid trees, *Abies* and Arboreal Pollen (%AP) from the CC09 record.

An interesting feature of AF demagnetization diagrams from beta and gamma zones is the systematic presence of gyroremanences over 35–40 mT characteristic of greigite (Fig. A.2D and F). The coexistence of this ferromagnetic sulfur with magnetite as the main magnetic carriers has been confirmed in the thermomagnetic curves (Fig. A.3A, C and D). The typical single-domain shape of the hysteresis cycles is also indicative of greigite (Fig. A.3B; Roberts et al., 2011). The identification of greigite has important implications from the paleomagnetic point of view since it is commonly reported as a product of diagenetic origin (e.g., Sagnotti et al., 2005; Porreca et al., 2009). In our case, however, the fact of having identified two magnetozones of opposite polarity but common magnetic properties (β and γ) does not point out to a remagnetization event. This indicates that the obtained paleomagnetic directions are really representative of the geomagnetic field and the remanence was acquired at the time (or shortly after) the deposition.

Furthermore, thermal demagnetization diagrams of the NRM in stratigraphic twin specimens from these magnetozones display the same polarity as their AF analogous (e.g., Fig. A.2D–E and F–H) pointing out that the determined paleomagnetic directions are not contaminated by the GRM effect. It is worth pointing out that polarity transitions identified in CC09 are not associated with any lithological change. Therefore, CC09 paleomagnetic record reveals a normal magnetic polarity interval between two of reverse polarity. Correlation of the observed polarity zonation with the Global Polarity Time Scale (GPTS; Gradstein et al., 2004) is discussed in Section 4.4.

### 3.2. Pollen analysis

The pollen record from the CC09 core shows high percentages of *Pinus* varying around and average value of 43% (Fig. 3). Other conifers such as *Abies*, *Cathaya*, *Tsuga*, *Cedrus*, *Picea*, *Larix/Pseudotsuga* and Taxodioideae (most likely *Taxodium* or *Glyptostrobus*) are also abundant in this record. *Engelhardia*, Taxodioideae and *Myrica* represent the most frequent thermophilous taxa. Temperate pollen species are dominated by *Quercus* (both evergreen and deciduous) but also *Alnus*, *Carpinus* (including *C.* cf. *orientalis*), *Carya*, *Liquidambar*, *Ulmus* and *Castanea–Castanopsis*. Typically Mediterranean taxa such as *Olea* and *Phillyrea*

occur frequently in the pollen samples. Cupressaceae s.l., Ericaceae and Poaceae are abundant in the pollen spectra. Aquatics, such as Cyperaceae also occur frequently in the pollen samples as well as the algae *Botryococcus*, which is sometimes very abundant.

One hundred and seven different pollen taxa have been identified in the CC09 core. The record shows a very rich and diverse flora, although many of the identified taxa occur in percentages lower than 1% (not plotted in Fig. 3). These rare species include thermophilous plants such as Arecaceae, *Croton*, Mimosaceae, *Prosopis*, Caesalpiniaceae, Sapotaceae, *Symplocos*, Cyrillaceae–Clethraceae, *Platycarya*, *Parthenocissus*, *Cissus*, Celastraceae, *Mussaenda*-type, *Microtropis fallax* and *Eucommia*. Temperate trees are also diversified and rare pollen species include *Aesculus*, *Fraxinus*, *Rhus*, *Ilex*, *Pterocarya*, *Juglans*, *Hamamelis*, *Parrotia*, Hamamelidaceae, *Platanus*, *Celtis*, *Populus* and *Ginkgo*.

Cluster analysis was run on the pollen data (excluding *Pinus*, as it is usually overrepresented) using the program CONISS (Grimm, 1987). This helped us, together with the pollen and algae percentages, to objectively zone the pollen data, producing six pollen zones for the CC09 record (Fig. 3). Even though there is a lot of variability in the pollen spectra, zones 1a, 2a and 3a are generally characterized by relatively high percentages in *Quercus* (both evergreen and deciduous), Poaceae, Ericaceae, Cupressaceae s.l., *Olea*, *Phillyrea* and Cyperaceae. On the other hand, during the deposition of zones 1b, 2b and 3b, arboreal pollen (%AP) dominated the pollen spectra including (besides *Pinus*) *Engelhardia*, *Abies*, *Cathaya*, *Tsuga*, *Larix*, *Castanea–Castanopsis* and *Alnus*. *Botryococcus* is also very abundant in these pollen spectra.

### 3.3. PCA analysis on the pollen data

PCA analysis on the pollen data shows two main groups of distinctive taxa (Fig. 4). One group, characterized by positive correlation to PC1 (PC1 +), is made up of Poaceae, *Quercus* (both evergreen and deciduous), Cupressaceae s.l., Oleaceae (*Olea*, *Phillyrea* and *Fraxinus*), Ericaceae, Cistaceae, Cyperaceae, *Corylus* and *Carpinus* cf. *orientalis*. The other main group, characterized by negative correlation to PC1 (PC1 —), is dominated by arboreal species and algae and includes *Engelhardia*, *Cathaya*, *Abies*, *Picea*, *Tsuga*, *Larix*, *Castanea–Castanopsis*, *Alnus*, *Zelkova* and *Botryococcus*. We could separate a third group, with negative correlation to both PC1 and PC2 that includes *Pinus* and *Cedrus*. PCA analysis indicates that Principal Component 1 (probably precipitation/seasonality see below) is strong, explaining the 98.763% of the variance.

Pollen data and cluster analysis agrees with the PCA analysis and pollen zones 1a, 2a and 3a are generally characterized by high relative abundances in the PC1+ pollen group and zones 1b, 2b and 3b are characterized by higher frequencies in the PC1—. *Pinus* and *Cedrus* seem to be more abundant during these later zones.

### 3.4. Periodicity of pollen and MS changes

Pollen data show a very clear cyclical pattern in the relative abundance of many taxa (Fig. 3). Cyclical variations are also observed in the lithology and MS, with alternations from darker (i.e., organic-rich) to lighter (i.e., organic-depleted) horizons (Fig. 2). Spectral analysis on the raw pollen data (most abundant pollen species from both PC1+ and PC1—) shows results with statistically significant (above the 80 and 90% confidence level) spectral peaks at periodicities between 2–3, 4, 7–8 and 15–20 m (Fig. 5). MS shows very similar results with significant spectral peaks at the above-mentioned frequencies (Fig. 5).

### 4. Discussion

#### 4.1. Late Pliocene vegetation and climate in the western Mediterranean area

Previous palynological studies on Pliocene sequences in the western Mediterranean area (Garraf 1 core; Suc and Cravatte, 1982; Tarragona E2 core; Bessais and Cravatte, 1988; Suc et al., 1995; Andalucía G1

core; Fauquette et al., 2007) show that vegetation was organized in altitudinal belts (Jiménez-Moreno et al., 2010). The following plant environments with their different species distribution have been described in this area: (1) a broad-leaved evergreen forest, from the coastal plains to about 700 m in altitude, mainly made up of *Taxodium* or *Glyptostrobus*, *Myrica*, *Rhus*, Theaceae, Cyrillaceae–Clethraceae, Euphorbiaceae, *Distylium*, evergreen *Quercus*, *Castanea–Castanopsis*, Sapotaceae, Rutaceae, Rubiaceae, *Mussaenda*, *Ilex*, *Hedera*, Oleaceae, Hamamelidaceae and *Engelhardia*; (2) an evergreen and deciduous mixed forest, above 700 m, characterized by deciduous *Quercus*, *Engelhardia*, *Platycarya*, *Carya*, *Pterocarya*, *Fagus*, *Liquidambar*, *Parrotia*, *Carpinus*, *Celtis*, *Acer*, etc. The shrub level was dominated by Ericaceae, *Ilex*, Caprifoliaceae, etc.; (3) between ca. 1000 and 1800 m, a mid-altitude deciduous and coniferous mixed forest occurred, with *Betula*, *Fagus*, *Cathaya*, *Cedrus* and *Tsuga* and (4) above 1800 m in altitude, a coniferous forest with *Abies* and *Picea* was present. Riparian vegetation was also identified, mainly composed of *Salix*, *Alnus*, *Carya*, *Zelkova*, *Ulmus* and *Liquidambar*.

The CC09 record is characterized by forested vegetation (AP between 57 and 97%). Pollen results from the CC09 core agree with previous studies from the western Mediterranean area (synthesis in Jiménez-Moreno et al., 2010), bearing taxa characteristic of all of the above-mentioned different vegetal environments (Fig. 3). The flora is very diverse, including many extinct thermophilous and hygrophilous species but also temperate taxa and high-elevation conifers (see Section 3.2; Fig. 3).

It is worth noting that typical Mediterranean-adapted taxa such as *Olea*, *Phillyrea* or evergreen *Quercus* were already quite abundant (pollen percentages up to 10% in Oleaceae total and evergreen *Quercus*) during the Late Pliocene in this area. The pollen abundance of Mediterranean sclerophyllous taxa in NE Spain during the Late Pliocene, with similar percentages as during the Holocene (Burjachs, 1994; Riera and Esteban, 1994; Burjachs and Schulte, 2003; Burjachs et al., 2005; Carrión et al., 2012), could indicate that this area was already under a certain seasonal Mediterranean climate. This agrees with Suc (1984) who observed a major reduction in subtropical taxa and an increase in sclerophyllous vegetation during the Late Pliocene, around 3.4 Ma (Suc and Popescu, 2005), establishing this age as the onset of the Mediterranean-type seasonal precipitation rhythm in the Mediterranean region.

*Artemisia* is very rare in this pollen record, which confirms that the sequence is older than 2.6 Ma and the beginning of the Pleistocene glaciations, when *Artemisia* steppes became widespread in this area (Jiménez-Moreno et al., 2010). Mid- and high-elevation conifers (*Cathaya*, *Cedrus*, *Tsuga*, *Larix*, *Abies*, *Picea*) are also quite abundant in this record. This indicates that these species occurred at higher elevation in the area, probably in the Catalan Coastal Ranges (i.e., Montseny peak, 1700 m, at 35 km to the SW) or the Pyrenees (i.e., Canigou Peak, 2785 m, ca. 80 km to the NW).

The occurrence of many thermophilous species (such as *Engelhardia* or Taxodioideae) points to a subtropical climate. Mean annual temperatures have been estimated around 1 to 5 °C warmer for the Late Pliocene in this area (Fauquette et al., 1998). Also the presence of many hygrophilous plants, living in SE China under high precipitation regimes, indicates mean annual precipitations 400 to 1000 mm higher than Present (Fauquette et al., 1998). The occurrence of hygrophilous species also indicates that, at that time, seasonality (in particular summer drought) was probably less marked than today (Jiménez-Moreno et al., 2009).

### 4.2. Vegetation changes and paleoecological implications

The CC09 pollen record shows the alternation of three relatively humid and arid periods. Climate during pollen zones 1a, 2a and 3a, which show relative increases in taxa belonging to PC1+, can be interpreted as relatively arid or characterized by a stronger seasonality. This can be deduced by the higher abundance in Mediterranean sclerophyllous xerophytes such as evergreen *Quercus*, *Olea*, *Phillyrea* and also Cupressaceae s.l. and grasses. Ericaceae has also been proven to increase with aridity in the western Mediterranean area (Pérez-

Obiol et al., 2011). The increase in Cyperaceae during these periods could indicate shallowing of the lake and an increase in shore and marsh surface area (Jiménez-Moreno et al., 2008). The driest periods in this area seem to be recorded during pollen zones 2a and 3a, reaching maxima in arid indicators. In addition, charcoal particles increased at these times, showing enhanced fire activity that was probably related with more aridity in the area (Whitlock and Anderson, 2003; Jiménez-Moreno et al., 2011). The lowest percentage in arboreal pollen and maximum in arid indicators (PC1+) occurred at ca. 25 m depth, during pollen zone 2a, recording a maximum in aridity (Figs. 3 and 7).

The opposite occurred during the deposition of zones 1b, 2b and 3b; arboreal trees (%AP) dominated the pollen spectra including (besides *Pinus*) *Engelhardia*, *Abies*, *Cathaya*, *Tsuga*, *Larix*, *Castanea–Castanopsis* and *Alnus* (all taxa belonging to PC1−). All these taxa probably grew at different elevations (see explanation above) but shared the same high-humidity requirements (or lack of strong seasonality). For example, *Abies* (sp.), probably an ancestor of *A. alba*, which occurs today in the Pyrenees, is associated with humid summers (*A. pinsapo*, its more meridional occurring relative is more adapted to summer drought; Alba-Sánchez et al., 2010). *Abies* forest developed at high elevation during humid interglacials in Greece (Ioannina 249; Tzedakis and Bennett, 1995). *Tsuga* also requires high precipitations (800–2000 mm), evenly distributed throughout the year, and unable to tolerate a dry summer season (Leroy and Roiron, 1996). *Engelhardia*, a semi-evergreen subtropical species typical of the broad-leaved evergreen forest in SE China (Wang, 1961) requires precipitation throughout the year (Jiménez-Moreno et al., 2005, 2009). *Botryococcus*, also very abundant in these pollen spectra, probably indicate deeper lake conditions and more productivity in the lake as has been deduced from other pollen records (Anderson et al., 2011).

The CC09 pollen record also shows long-term trends in the abundance of significant pollen taxa. For example, %AP, and in particular *Abies*, is characterized by a progressive decreasing trend towards the top of the record (Fig. 7). Arid taxa seem to show the opposite trend, with increasing values towards the top. This could be related to a long-term increasing trend in aridity. An increase in aridity has also been observed in other pollen records from the area (Fauquette et al., 1998) through a long-term decrease in thermophilous/hygrophilous taxa and an increase in Mediterranean xerophytes and herbs during the Late Pliocene (between ca. 3.56 and 3.22 Ma). This also agrees with more recent data from marine cores from the Mediterranean and Atlantic Ocean that show an intensification of the Mediterranean outflow around 3.5–3.2 Ma related with an increase in seasonal aridity (Khélifi et al., 2009).
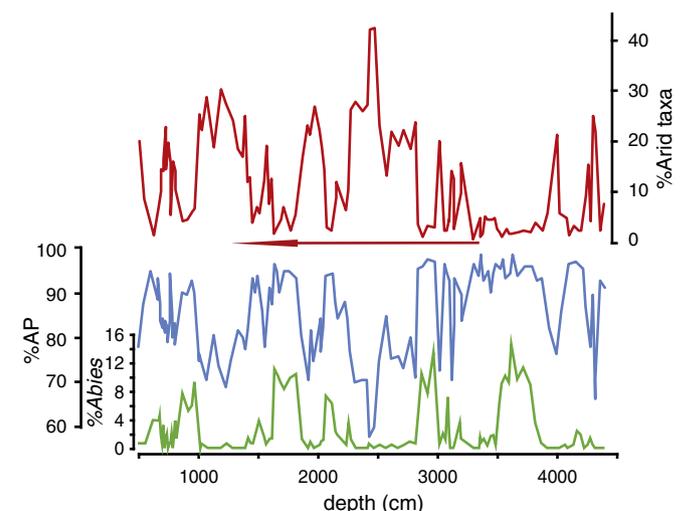


Fig. 7. Comparison of the percentages of *Abies*, Arboreal Pollen (AP) and arid taxa (PC1+ group see text for explanation) from the CC09 record. The arrow points to an aridification trend.

## 4.3. Vegetation succession

High-resolution pollen studies show very detailed vegetal succession patterns during climate change. For example, during glacial–interglacial cycles pollen diagrams from southern Europe show a pre-temperate (late glacial) phase of open woodland (with *Juniperus*, *Pinus*, *Betula*, deciduous *Quercus*). Later on, the onset of the interglacial is characterized by early expansion of Mediterranean sclerophylls and deciduous *Quercus*. This is followed by a decrease in Mediterranean sclerophylls and an expansion in deciduous trees and the final part of the interglacial is characterized by late successional trees (conifers such as *Abies* and *Picea*) and increases in herbs (synthesis in Tzedakis, 2007). These successional patterns in the vegetation have also been described for the Pliocene and early Pleistocene (Combourieu-Nebout, 1993; Bertini, 2001; Joannin et al., 2007; Leroy et al., 2011; Fig. 8). Climate during the Pliocene was warmer (Zachos et al., 2001) than during the Pleistocene and subtropical vegetation also forms part of this succession. Therefore, the Pliocene "glacial–interglacial" cycles in the Mediterranean area were characterized by the succession of four main vegetal assemblages (see Bertini, 2001 for synthesis): deciduous forest, subtropical/warm-temperate forest, altitudinal conifer forest and open vegetation. This succession evidences four main climatic conditions: a first increase in temperature followed by an increase in humidity; a decrease in temperature without variations of humidity and finally a strong decrease in humidity, corresponding to a gradual transition from warm and humid conditions during interglacials to cold and dry conditions during glacials (Fig. 8). These four phases are not always evident in the high-resolution pollen records and a pollen record from Stirone, Italy shows that phases dominated by a herbaceous vegetation are lacking whereas an important increase of altitudinal conifers, in particular *Picea*, is recorded. This was interpreted as local climatic conditions that favored the development of a high-elevation conifer forest instead of steppic grasses in the area during glaciations (Bertini, 2001).

The CC09 pollen record shows covariation of plant species that live today at very different environments (i.e., elevations). This is the case of low-altitude subtropical species such as *Engelhardia* and high-altitude conifers such as *Abies*. These two species seem to covary almost synchronously throughout the record. The same applies to herbs and, for example, evergreen and deciduous *Quercus*. In the CC09 record we mostly see changes related to humidity and we were only able to distinguish two of the four phases of the glacial–interglacial vegetal succession described above: a humid phase including the subtropical and humid forest together with the altitudinal conifer forest and an arid phase characterized by open vegetation and deciduous forest (Fig. 8). *Pinus* and *Cedrus* seem to increase at the transitions between those two main phases, leading to higher elevation or more hygrophilous conifers (Fig. 9).

## 4.4. CC09 core magnetochronology

The coexistence of *S. jeanvireti* and *A. tigneresi* suggests an age of about 3.2 Ma (Late Pliocene) for the Camp dels Ninots sedimentary sequence, near the MN15–MN16 mammal biozone transition (Gómez de Soler et al., 2012; see Section 4.6 on MN units). The correlation of paleomagnetic results with the GPTS (Fig. 10) as well as with the referred paleontological data, suggest that the normal to reverse polarity transition identified between gamma (γ) and beta (β) magnetozones corresponds to the transition between subchron C2An.2n [3.11–3.22 Ma] and C2An.1r (Kaena) [3.04–3.11 Ma]. Following this line of interpretation, the reversed interval identified at delta (δ) zone would thus equate to the Mammoth subchron (C2An.2r) [3.22–3.33 Ma]. An alternative explanation would be the correlation of the lowest reverse interval (δ zone) with the C2Ar chron (Gilbert) whose best age estimation is between 3.58 and 4.18 Ma (Gradstein et al., 2004). Consequently, this would imply that the gamma zone would correlate to C2An.3n (3.33–3.58 Ma) and the beta zone to C2An.2r (Mammoth subchron). This latter interpretation, however, does not fit well with sedimentological and
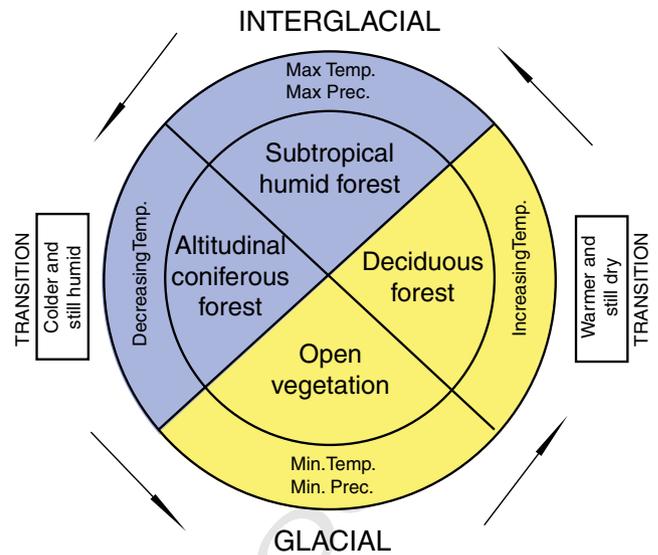


**Fig. 8.** Vegetation succession during an ideal "glacial–interglacial" cycle during the Late Pliocene and Early Pleistocene. Arrows point to the direction of the change. In yellow and blue the arid and humid phases respectively identified in this study.
Modified from Combourieu-Nebout (1993) and Bertini (2001).

cyclostratigraphical evidences (see below) or the biostratigraphic data, which indicate an age of ca. 3.2 Ma for the faunal assemblage (Gómez de Soler et al., 2012) documented in the upper part of the sequence.

## 4.5. Astronomical forcing on vegetation and sedimentation

The palynological results from CC09 core show a very clear cyclical pattern in the vegetation. Cycles are characterized by the alternation of dominantly hygrophilous (PC1−) vs. xerophilous (PC1+) plants (see above for explanation; Fig. 6). Different scale cyclicities can be observed visually within the different pollen zones (Figs. 3, 6 and 7). The main driver triggering vegetation changes in this area seemed to be precipitation. Humid periods are characterized by %AP between 90 and 97% and arid periods by around 70%. The magnitude of the oscillations is much lower than between Pleistocene glacial–interglacial cycles, when %AP can reach up to values close to 0% during glaciations (i.e., Tenaghi Philippon; Tzedakis, 2007). Therefore, orbital-scale climate variability was less pronounced during the Late Pliocene than during the last 2.6 Ma in the Mediterranean area.

Spectral analysis of the pollen data identified cycles with periodicities at 2–3, 4, 7–8 and 15–20 m in the studied sequence (Fig. 5). As the studied core lacks a detailed chronological control we cannot directly assign these periodicities to a certain time period (i.e., orbital cycle). However, we can estimate their time duration making a few assumptions, supported by the biostratigraphic and paleomagnetic data, and knowing what really triggers vegetation changes in the study area. One of the most statistically significant cyclicities has a periodicity of ca. 4 m and can be identified in the most significant humid and arid indicators as well as in the %AP and MS (Fig. 5). Humid taxa data were filtered at a 4 m frequency (0.0025 frequency and 0.001 bandwidth) and the resulting plot explains most of the variability observed (Fig. 6). In the Mediterranean area, cyclical changes in the vegetation are mostly forced by precession (Kloosterboer-van Hoeve et al., 2006; Tzedakis, 2007; Sánchez Goñi et al., 2008). If we consider the 4 m cycle forced by precession (21 ka), the 7.5 m cyclicity would correspond to ca. 40 ka (obliquity) and the 17.5 (15–20) m to ca. 90 ka (79–105 ka; eccentricity) producing a perfect orbital-scale fit for the observed spectral peaks. The 2–3 m (10.5–15.7 ka) cycle could then be related to a mix of a half-precession harmonic (ca. 10–12 ka) with the 19 ka precession orbital component. Following this, the calculated sedimentary rate for
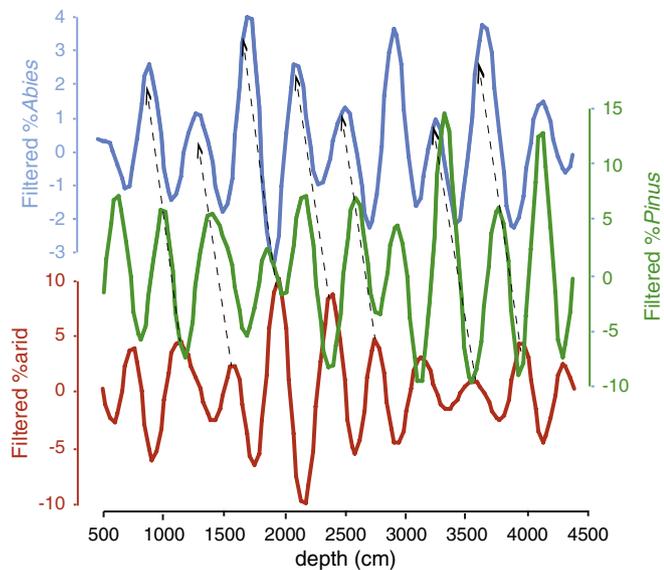
Fig. 9. Comparison of the 4-m filtered arid taxa, *Pinus* and *Abies* from the CC09 core record. Arrows point to the direction of the vegetation succession.

this sequence would be of ca. 0.19 mm/yr, which agrees with average values in other maar environments (for example 0.14 mm/yr in Messel maar, Germany, Lenz et al., 2010).



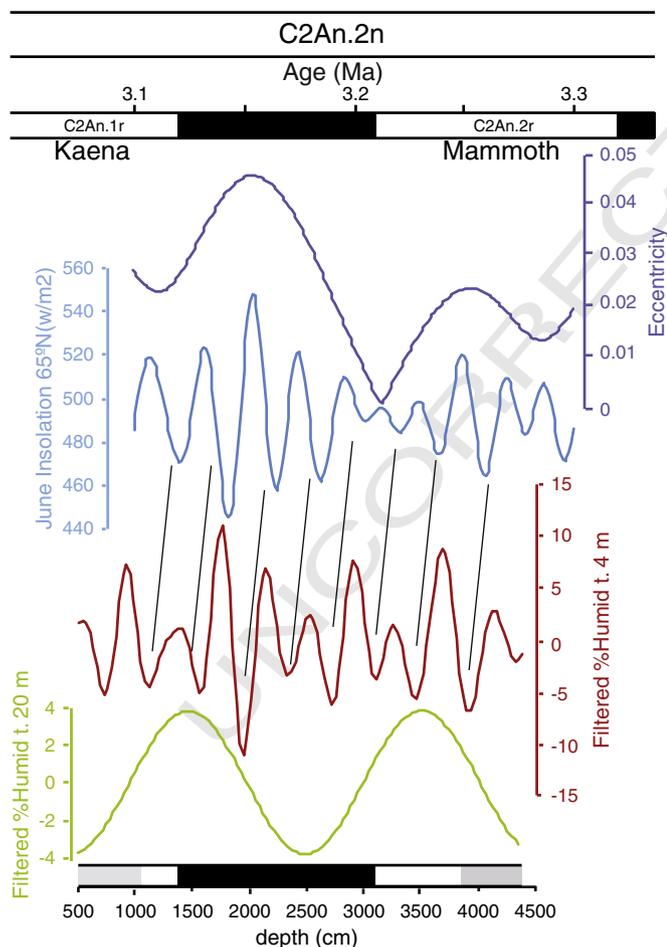Fig. 10. Correlation of the magnetozones, 20- and 4-m filtered humid taxa from CC09 core with the eccentricity (Laskar et al., 2004), summer insolation at 65°N (Laskar et al., 2004) and reference paleomagnetic data (ATNTS04; Lourens et al., 2004) between 3.3 and 3.1 Ma. The normal chrons shown are part of the Gauss chron. Note that the minimum in humidity at ca. 25 m would correlate with the minima in eccentricity at ca. 3.2 Ma.

The paleomagnetic data support these sedimentary rate estimations. The normal polarity interval identified in the middle of the lacustrine facies, taking into account the biostratigraphic age given by mammals of ca. 3.2 Ma, could be most-likely assigned to the Gauss chron 2An.2n (3.20–3.11 Ma; ATNTS04), sandwiched by two reversals: Mammoth and Kaena. Our pollen results fully support this assignment: this normal chron has an estimated duration of 90 ka (ATNTS04) and in the CC09 pollen record this time period is characterized by four complete precession cycles, which gives us a very similar duration of the normal chron of ca. 84 ka (4 ∗ 21 ka) (Fig. 10).

The plots obtained by filtering the % humid taxa at the frequencies of the precession (explained above), obliquity (7.5 m; 0.0013 frequency and 0.001 bandwidth) and eccentricity (20 m; 0.0005 and 0.001 bandwidth) explain all the variability observed in the CC09 pollen record (Fig. 6). A good match in amplitude variation is found between the astronomical forcing and the filtered outputs (Fig. 10). Following this, the studied sequence would have been deposited in ca. 200 ka. Our record shows a minimum in precipitation (maximum in arid indicators and charcoal) around 25 m depth that was probably triggered by low-amplitude insolation minima and eccentricity minima (Fig. 10). Also, the highest MS occurred at that time with roughly less organic sedimentation in the lake. Lithology and MS show that dark mudstones, probably organic-rich, occurred during precipitation maxima (Fig. A.4). This coincides with marine records from the Mediterranean that show that sapropels were deposited during humid periods related with insolation maxima (precession minima; Rossignol-Strick, 1983; Hilgen, 1991). MS variations would mostly be related to changes in organic productivity in the lake, anoxic conditions, etc.

Even though several studies show the important role of obliquity in shaping the vegetation during the 2.8–1.0 Ma period (Klotz et al., 2006; Joannin et al., 2008; Leroy, 2008; Popescu et al., 2010; Suc et al., 2010), there is not much information about obliquity forcing on the vegetation earlier in the Pliocene in this area. For example, Popescu (2001) recorded spectral peaks related with obliquity in an early Pliocene pollen record (Lupoaia, Romania) but no further discussion can be found in that paper. The CC09 record shows that obliquity is also important at that time in shaping the vegetation. This reflects a high-latitude influence on the Mediterranean climate through changes in seasonal contrast, mostly controlling temperature variations (Tuenter et al., 2003; Suc et al., 2010).

### 4.6. Mammal biostratigraphical implications

The MN (Mammal Neogene) units, with age estimates by Agustí et al. (2001), are commonly used in continental biostratigraphy (Mein, 1975, 1990; De Bruijn et al., 1992). The large mammals found at Camp dels Ninots include *S. jeanvireti*, a rare rhinoceros that is only known from MN16, and *Alephis*, a large bovid which in western Europe was replaced by *Leptobos* late in MN15 or around the MN15–16 transition, while in south-eastern Europe it may have survived later. In a broad sense, these mammals pointed to an age close to the MN15–16 transition, around 3.2 Ma (Gómez de Soler et al., 2012). The combination of paleomagnetism and cyclostratigraphy suggests that chron C2An.2n is present in the CC09 core. The large mammal fossils come from nearby sediments that can be correlated to the upper part of the studied core (see correlations in Figs. 2 and A.1), implying that they date to the Kaena subchron (C2An.1r, 3.03–3.11 Ma; or to an even younger chron). Therefore, rough age estimation for the paleontological site of ca. 3.06 Ma could be suggested by combining the 0.19 mm/yr accumulation rate and the distance between the site and the Kaena base reversal (10.5 m and 3.116 Ma, respectively). Anyway, only an age younger than Kaena base reversal can be assured from a combined magnetobiostratigraphic point of view.

The reference localities for MN15 and 16 are Perpignan in France and Arondelli/Triversa in Italy. About 20 m below the site of Serrat d'en Vacquer at Perpignan, the Gilbert Chron (C2Ar) was detected, while the Triversa fauna in the RDB quarry is correlated to the C2An.2n unit

just below the Kaena Subchron (=C2An.1r) (Steininger et al., 1996). This implies that the MN15–16 transition should be roughly between 3.6 and 3.2 Ma. More recently, in Spain the MN15–16 transition was dated to around 3.2 Ma (Agustí et al., 2001). The locality Las Higueruelas (Ciudad Real, Spain) is in a similar volcanic setting as Camp dels Ninots and has been dated to either the Kaena or Mammoth Subchrons (Mazo, 1999). In view of the age of the MN15–16 transition, this locality dates probably to the Kaena Subchron. Large mammals that arrived by dispersal into western Europe around the MN15–16 transition include *Leptobos* and *Acinonyx* (present in Arondeli; De Bruijn et al., 1992) and *Arvernoceros*, *Cervus perrieri* and *Stephanorhinus etruscus* (present in Las Higueruelas; Mazo, 1999). If all datings and identifications are correct, this implies that *Alephis* from Camp dels Ninots postdates the earliest *Leptobos* in western Europe and was very close to, possibly even younger than, the arrivals of several other MN16 elements. At least in western Europe, the latest record of *Alephis* is from Camp dels Ninots.

## 5. Conclusions

A multiproxy analysis of a sediment core from the Late Pliocene Camp dels Ninots maar, allowed us to reconstruct the vegetation, sedimentation and climate variability, around 3.2 Ma in NE Spain. Through comparing this study with other records from the Mediterranean area we obtained the following main conclusions:

(1) Pollen data indicate that during the Late Pliocene a very diverse flora existed in NE Spain including subtropical, temperate and Mediterranean taxa.
(2) Vegetation was very similar to previous studies and indicates a relatively humid subtropical climate with certain seasonality.
(3) A progressive aridification is observed, which agrees with other Late Pliocene global climatic records.
(4) We observed the presence of a clear climate cyclicity that forced both the vegetation and sedimentation in the Camp dels Ninots maar. These cycles are mostly humid–arid (or less–more seasonality) and are mostly forced by precession but also by obliquity and eccentricity.
(5) The studied sedimentary sequence was deposited in 200 ka (3.3–3.1 Ma).

## 6. Uncited references

Carrancho et al., 2012
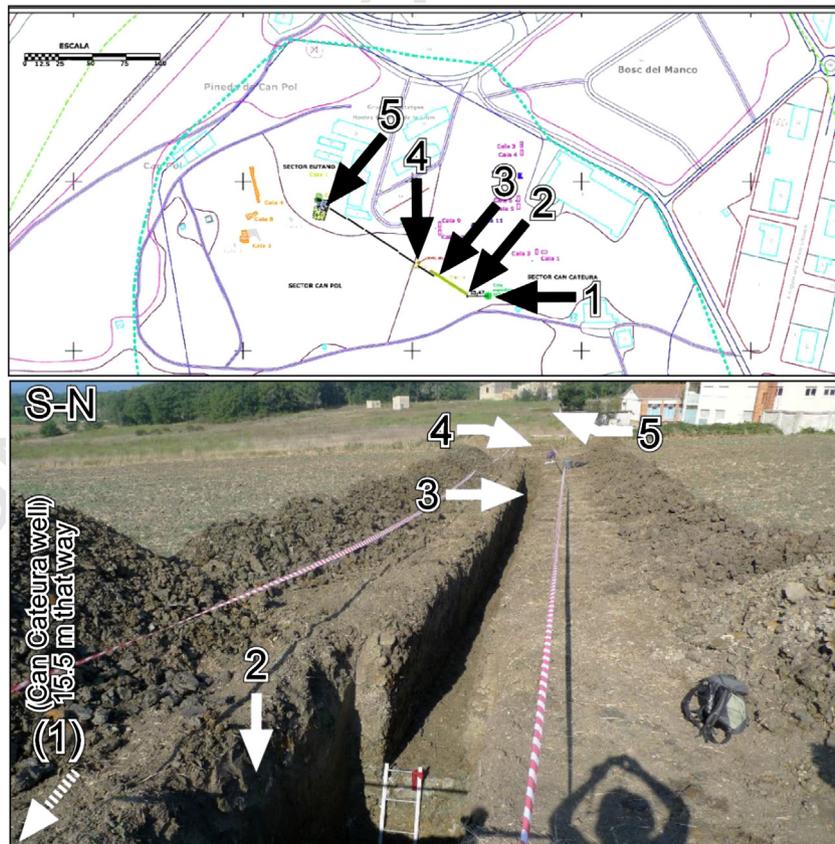Beaver et al., 2005

## Appendix 1



**Figure Appendix 1.** Location of sedimentary outcrops described in the text and Fig. 2. The photo shows how the correlation between the mammal sites and the CC09 core was done (see Fig. 2).
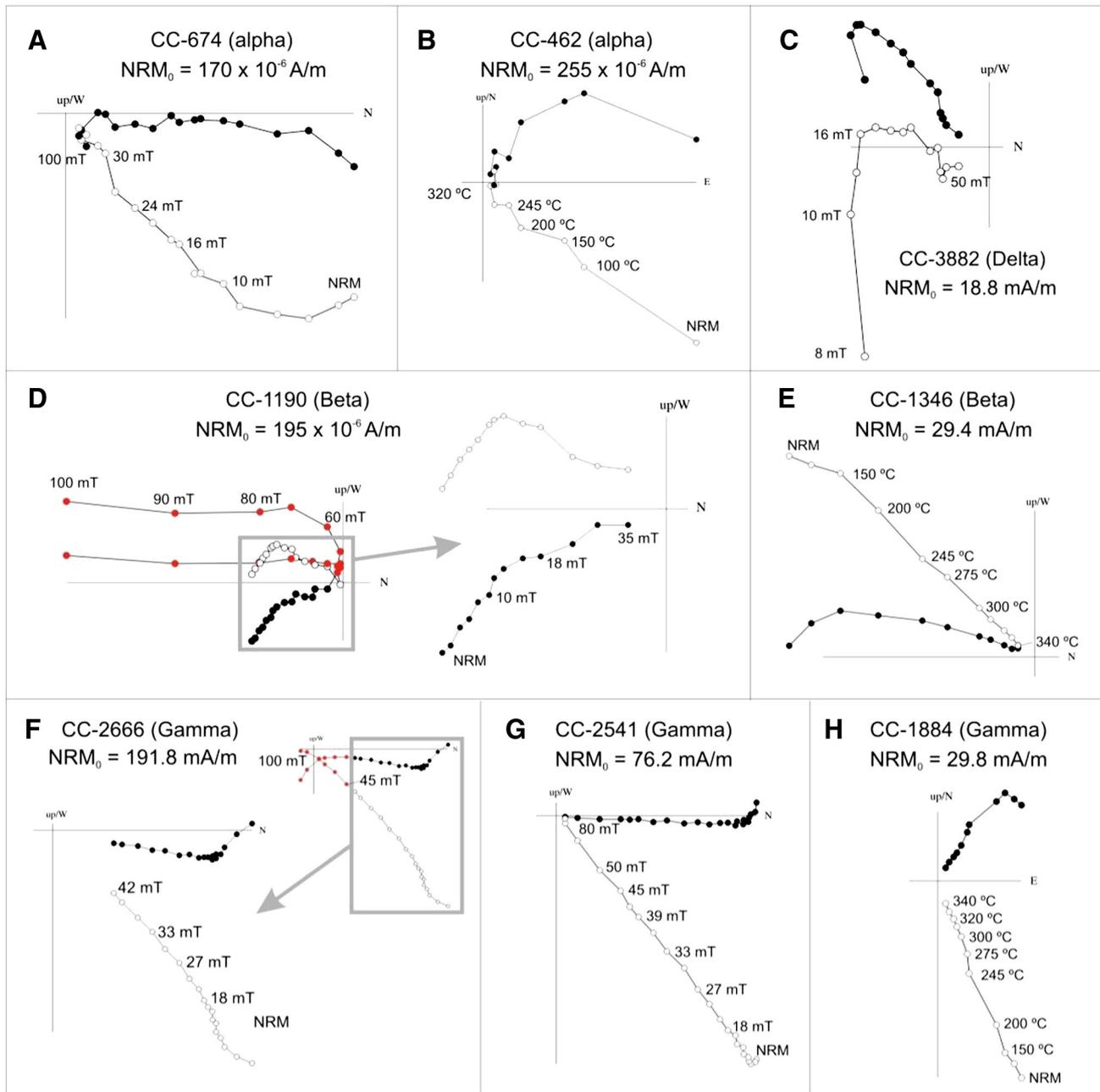
**Figure Appendix 2.** Orthogonal NRM demagnetization plots for representative samples from CC09. (A, C, D, F and G) Samples demagnetized by alternating fields. (B, E and H) Samples thermally demagnetized. Closed (open) symbols show projections of vector endpoints onto the horizontal (vertical) plane. Sample code, magnetozone and initial intensity ($NRM_0$) are indicated for each sample. Insets of panels d and f show the plots without the contribution of gyroremanences (red circles).
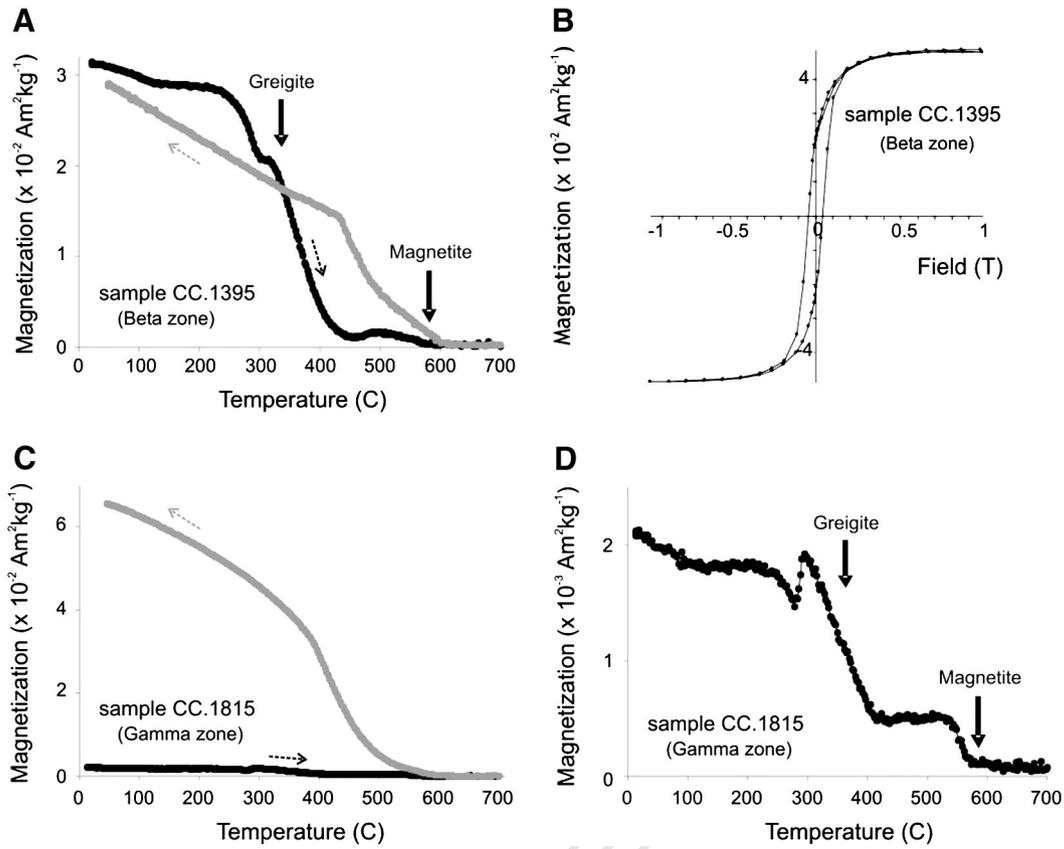
**Q8**  **Figure Appendix 3.** (A, B and D). Representative thermomagnetic curves from (A) beta and (C–D) gamma zones. (B) Hysteresis loop corresponding to the same sample plotted in panel A. Heating (cooling) cycles are represented in black (gray) and denoted by dashed arrows. Magnetization intensity values, sample code, stratigraphic zone and the inflection corresponding to the ferromagnetic mineral phases indicated are also represented.
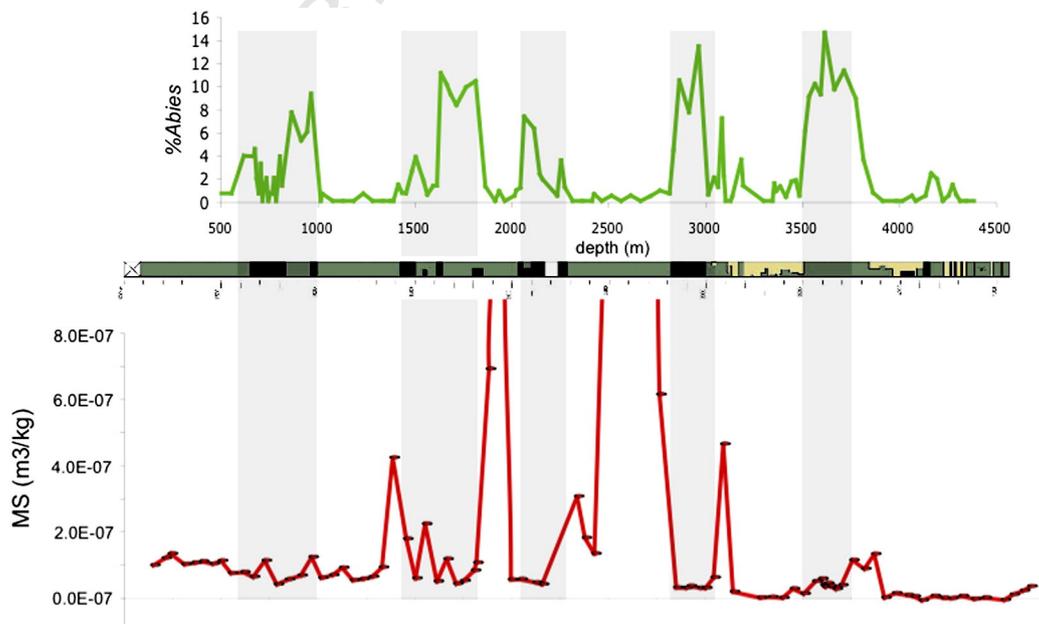


**Figure Appendix 4.** Comparison of the magnetic susceptibility (MS), lithology and pollen record (%Abies) from the CC09 core. Gray shadings indicate humid periods that generally correspond to dark clays and low MS.

## References

Agustí, J., Cabrera, L., Garcés, M., Krijgsman, W., Oms, O., Parés, J.M., 2001. A calibrated mammal scale for the Neogene of Western Europe. State of the art. Earth-Science Reviews 52, 247–260.

Alba-Sánchez, F., López-Sáez, J.A., Benito-de Pando, B., Linares, J.C., Nieto-Lugilde, D., López-Merino, L., 2010. Past and present potential distribution of the Iberian *Abies* species: a phytogeographic approach using fossil pollen data and species distribution models. Diversity and Distributions 16, 214–228.

Anderson, R.S., Jiménez-Moreno, G., Carrión, J.S., Pérez-Martínez, C., 2011. Postglacial history of alpine vegetation, fire and climate from Laguna de Río Seco, Sierra Nevada, southern Spain. Quaternary Science Reviews 30, 1615–1629.

Barrón, E., Rivas-Carballo, R., Postigo-Mijarra, J.M., Alcalde-Olivares, C., Vieira, M., Castro, L., Pais, J., Valle-Hernández, M., 2010. The Cenozoic vegetation of the Iberian Peninsula: a synthesis. Review of Palaeobotany and Palynology 162, 382–402.

Bertini, A., 2001. Pliocene climatic cycles and altitudinal forest development from 2.7 Ma in the Northern Apennines (Italy): evidence from the pollen record of the Stirone section (−5.1 to −2.2 Ma). Geobios 34, 253–265.

Bessais, E., Cravatte, J., 1988. Les écosystèmes végétaux Pliocènes de Catalogne méridionale. Variations latitudinales dans le domaine Nord-Ouest méditerranéen. Geobios 21, 49–63.

Beug, H.-J., 2004. Leitfaden del pollenbestimmung für mitteleuropa und angrenzende gebiete.Pfeil, München (542 pp.).

Burjachs, F., 1994. The palynology of the Upper Pleistocene and Holocene of the North-East Iberian Peninsula: Pla de L'Estany (Catalonia). Historical Biology 9 (1–2), 17–33.

Burjachs, F., Schulte, L., 2003. El paisatge vegetal del Penedès entre la Prehistòria i el Món Antic. In: Guitart, J., Palet, J.M., Prevosti, M. (Eds.), Territoris antics a la Mediterrània i a la Cossetània oriental: 249–254. Departament de Cultura, Generalitat de Catalunya, Barcelona.

Burjachs, F., López-Sáez, J.A., Iriarte, M.J., 2003. Metodología arqueopalinológica. In: Buxó, R., Piqué, R. (Eds.), La recogida de muestras en arqueobotànica: objetivos y propuestas metodológicas. Museu d'Arqueologia de Catalunya − Barcelona, Barcelona, pp. 11–18.

Burjachs, F., Bach, J., Buxó, R., Llàcer, P., McGlade, J., Picazo, M., Piqué, R., Ros, M.T., 2005. El territori d'Emporion i les seves dades paleoambientals. Empúries 54, 21–28.

Carrancho, A., Villalaín, J.J., Gómez de Soler, B., Campeny-Vallosera, G., Oms, O., Agustí, J., van der Made, J., Blain, H.-A., Burjachs, F., Jiménez-Moreno, G., Expósito, I., Barrón, E., 2012. Estudio paleomagnético preliminar de una sucesión lacustre pliocena en la Depresión de la Selva (Cordilleras Costero Catalanas, NE Península Ibérica). Geotemas 13, 1136–1139.

Carrión, J.S., Fernández, S., González Sampériz, P., López Merino, L., Peña, L., Burjachs, F., López-Sáez, J.A., García-Antón, M., Carrión Marco, Y., Uzquiano, P., Postigo, J.M., Barrón, E., Allué, E., Badal, E., Dupré, M., Fierro, E., Munuera, M., Rubiales, J.M., García Amorena, I., Jiménez-Moreno, G., Gil Romera, G., Leroy, S., García Martínez, M.S., Montoya, E., Fletcher, W., Yll, E., Vieira, M., Rodríguez Ariza, M.O., Anderson, S., Peñalba, C., Gil García, M.J., Pérez Sanz, A., Albert, R.M., Díez, M.J., Morales, C., Gómez Manzaneque, F., Parra, I., Ruiz Zapata, B., Riera, S., Zapata, L., Ejarque, A., Vegas, T., Rull, V., Scott, L., Andrade, A., Pérez Díaz, S., Abel Schaad, D., Moreno, E., Hernández Mateo, L., Sánchez Baena, J.J., Riquelme, J.A., Iglesias, R., Franco, F., Chaín, C., Figueiral, I., Grau, E., Matos, M., Jiménez Espejo, F., Arribas, A., Garrido, G., Finlayson, G., Finlayson, C., Ruiz, M., Pérez Jordá, G., Miras, Y., 2012. Paleoflora y Paleovegetación de la Península Ibérica e Islas Baleares: Plioceno–Cuaternario. Ministerio de Economía y Competitividad, Madrid (e-book. [http://www.paleofloraiberica.net/INICIO.html]).

Combourieu Nebout, N., Foucault, A., Mélières, F., 2004. Vegetation markers of palaeoclimate cyclical changes in the Pliocene of Punta Piccola (Sicily, Italy). Palaeogeography, Palaeoclimatology, Palaeoecology 214, 55–66.

Combourieu-Nebout, N., 1993. Vegetation response to Upper Pliocene glacial/interglacial cyclicity in the Central Mediterranean. Quaternary Research 4, 228–236.

de Bruijn, H., Daams, R., Daxner-Höck, G., Fahlbusch, V., Ginsburg, L., Mein, P., Morales, J., Heizmann, E., Mayhew, D.F., Van der Meulen, A.J., Schmidt-Kittler, N., Telles Antunes, M., 1992. Report of the RCMNS working group on fossil mammals, Reisenburg 1990. Newsletters on Stratigraphy 26 (2–3), 65–118.

Faegri, K., Iversen, J., 1989. Textbook of Pollen Analysis.Wiley, New York.

Fauquette, S., Guiot, J., Suc, J.-P., 1998. A method for climatic reconstruction of the Mediterranean Pliocene using pollen data. Palaeogeography, Palaeoclimatology, Palaeoecology 144, 183–201.

Fauquette, S., Suc, J.-P., Jiménez-Moreno, G., Micheels, A., Jost, A., Favre, E., Bachiri-Taoufiq, N., Bertini, A., Clet-Pellerin, M., Diniz, F., Farjanel, G., Feddi, N., Zheng, Z., 2007. Latitudinal climatic gradients in Western European and Mediterranean regions from the Mid-Miocene (15 Ma) to the Mid-Pliocene (3.5 Ma) as quantified from pollen data. In: Williams, M., Haywood, A.M., Gregory, F.J., Schmidt, D.N. (Eds.), Deep-Time Perspectives on Climate Change: Marrying the Signal from Computer Models and Biological Proxies. The Micropalaeontological Society, Special Publications. The Geological Society, London, pp. 481–502.

Galán, L., Vegas, J., García-Cortés, A., 2009. Reconstrucción paleoclimática del centro de la Península Ibérica durante los últimos 50 ka cal. BP, a partir de los datos físicos y geoquímicos del registro lacustre del maar de Fuentillejo (Campo de Calatrava, Ciudad Real). Geogaceta 46, 119–122.

Goeury, Cl, Beaulieu, J.-L. De, 1979. À propos de la concentration du pollen à l'aide de la liqueur de Thoulet dans les sédiments minéraux. Pollen et Spores 11 (1–2), 239–251.

Gómez de Soler, B., Campeny Vall-Llosera, G., van der Made, J., Oms, O., Agustí, J., Sala, R., Blain, H.A., Burjachs, F., Claude, J., García Catalán, S., Riba, D., Rosillo, R., 2012. The Camp dels Ninots (NE Spain): a new key locality for the Middle Pliocene terrestrial faunas of Europe. Geologica Acta 10 (2), 1–17.

Gradstein, F., Ogg, J., Smith, A., 2004. A Geologic Time Scale.Cambridge University Press (588 pp.).

Grimm, E.C., 1987. CONISS: a Fortran 77 program for stratigraphically constrained cluster analysis by the method of incremental sum of squares. Computers and Geosciences 13, 13–35.

Hammer, O., Harper, D.A.T., Ryan, P., 2001. Past: paleontological statistics software package for education and data analysis. Palaeontologia Electronica 4 (1) (art. 4, 9 pp.).

Hilgen, F.J., 1991. Astronomical calibration of Gauss to Matuyama sapropels in the Mediterranean and implication for the geomagnetic polarity time scale. Earth and Planetary Science Letters 104, 226–244.

Intergovernmental Panel on Climate Change (IPCC), 2007. In: Solomon, S., et al. (Ed.), Climate Change 2007: The Physical Science Basis—Contribution of Working Group I to the Fourth Assessment Report of the Intergovernmental Panel on Climate Change. Cambridge Univ. Press, New York (996 pp.).

Jiménez-Moreno, G., Rodríguez-Tovar, F.-J., Pardo-Igúzquiza, E., Fauquette, S., Suc, J.-P., Müller, P., 2005. High-resolution palynological analysis in late Early–Middle Miocene core from the Pannonian Basin, Hungary: climatic changes, astronomical forcing and eustatic fluctuations in the Central Paratethys. Palaeogeography, Palaeoclimatology, Palaeoecology 216 (1–2), 73–97.

Jiménez-Moreno, G., Fawcett, P.J., Anderson, R.S., 2008. Millennial- and centennial-scale vegetation and climate changes during the Late Pleistocene and Holocene from northern New Mexico (USA). Quaternary Science Reviews 27, 1442–1452.

Jiménez-Moreno, G., de Leeuw, A., Mandic, O., Harzhauser, M., Pavelic, D., Krijgsman, W., Vranjkovic, A., 2009. Integrated stratigraphy of the Early Miocene lacustrine deposits of Pag Island (SW Croatia): palaeovegetation and environmental changes in the Dinaride Lake System. Palaeogeography, Palaeoclimatology, Palaeoecology 280, 193–206.

Jiménez-Moreno, G., Suc, J.-P., Fauquette, S., 2010. Miocene to Pliocene vegetation reconstruction and climate estimates in the Iberian Peninsula from pollen data. Review of Palaeobotany and Palynology 162, 403–415.

Jiménez-Moreno, G., Anderson, R.S., Atudorei, V., Toney, J.L., 2011. A high-resolution record of vegetation, climate, and fire regimes in the mixed conifer forest of northern Colorado (USA). Geological Society of America Bulletin 123, 240–254.

Joannin, S., Quillévéré, F., Suc, J.-P., Lécuyer, C., Martineau, F., 2007. Early Pleistocene climate changes in the central Mediterranean region as inferred from integrated pollen and planktonic foraminiferal stable isotope analyses. Quaternary Research 67, 364–374.

Joannin, S., Ciaranfi, N., Stefanelli, S., 2008. Vegetation changes during the late early Pleistocene at Montalbano Jonico (Province of Matera, southern Italy) based on pollen analysis. Palaeogeography, Palaeoclimatology, Palaeoecology 270, 92–101.

Khélifi, N., Sarnthein, M., Andersen, N., Blanz, T., Frank, M., Garbe-Schönberg, D., Haley, B.A., Stumpf, R., Weinelt, M., 2009. A major and long-term Pliocene intensification of the Mediterranean outflow 3.5–3.3 Ma ago. Geology 37, 811–814.

Kloosterboer-van Hoeve, M.L., Steenbrink, J., Visscher, H., Brinkhuis, H., 2006. Millennial-scale climatic cycles in the Early Pliocene pollen record of Ptolemais, northern Greece. Palaeogeography, Palaeoclimatology, Palaeoecology 229, 321–334.

Klotz, S., Fauquette, S., Combourieu-Nebout, N., Uhl, D., Suc, J.-P., Mosbrugger, V., 2006. Seasonality intensification and long-term winter cooling as a part of the Late Pliocene climate development. Earth and Planetary Science Letters 241, 174–187.

Laskar, J., Robutel, P., Joutel, F., Gastineau, M., Correia, A.C.M., Levrard, B., 2004. A long term numerical solution for the insolation quantities of the Earth. Astronomy and Astrophysics 428, 261–285.

Lenz, O.K., Wilde, V., Riegel, W., Harms, F.-J., 2010. A 600 k.y. record of El Niño–Southern Oscillation (ENSO): evidence for persisting teleconnections during the Middle Eocene greenhouse climate of Central Europe. Geology 38, 627–630.

Leroy, S.A.G., 2008. Vegetation cycles in a disturbed sequence around the Cobb–Mountain subchron in Catalonia. Journal of Paleolimnology 40 (3), 851–868.

Leroy, S.A.G., Dupont, L., 1994. Development of vegetation and continental aridity in northwestern Africa during the Late Pliocene: the pollen record of ODP Site 658. Palaeogeography, Palaeoclimatology, Palaeoecology 109, 295–316.

Leroy, S.A.G., Roiron, P., 1996. Latest Pliocene pollen and leaf floras from Bernasso palaeolake (Escandorgue Massif, Hérault, France). Review of Palaeobotany and Palynology 94, 295–328.

Leroy, S.A.G., Zolitschka, B., Negendank, J.F.W., Seret, G., 2000. Palynological analyses in the laminated sediment of Lake Holzmaar (Eifel, Germany): duration of Lateglacial and Preboreal biozones. Boreas 29, 52–71.

Leroy, S.A.G., Arpe, K., Mikolajewicz, U., 2011. Vegetation context and climatic limits of the Early Pleistocene hominid dispersal in Europe. Quaternary Science Reviews 30, 1448–1463.

Lindner, H., Gabriel, G., Götze, H.-J., Kaeppler, R., Suhr, P., 2006. Geophysical and geological investigation in the Upper Lusatia region (East Saxony). Zeitschrift der Deutschen Gesellschaft für Geowissenschaften 157 (3), 355–372.

Loublier, Y., 1978. Application de l'analyse pollinique à l'étude du paléoenvironnement du remplissage Würmien de la grotte de L'Arbreda (Espagne). Académie de Montpellier (U.S.T.L.), Montpellier.

Lourens, L.J., Hilgen, F.J., Laskar, J., Shackleton, N.J., Wilson, D., 2004. The Neogene period. In: Gradstein, F.M., Ogg, J.G., Smith, A.G. (Eds.), A Geological Time Scale 2004. Cambridge University Press, Cambridge, pp. 409–440.

Mazo, A.V., 1999. Vertebrados fósiles del Campo de Calatrava (Ciudad Real). In: Aguirre, E., Rábano, I. (Eds.), La Huella del Pasado Fósiles de Castilla-La Mancha. Patrimonio Histórico. Arqueología Castilla la Mancha. Junta de Comunidades Castilla–La Mancha–Toledo, pp. 281–296.

Mein, P., 1975. Proposition de biozonation du Néogène méditerranéen à partir des mammifères. Trabajos sobre Neógeno-Cuaternario 4, 112.

Mein, P., 1990. Updating of MN zones. In: Lindsay, E.H., Fahlbusch, V., Mein, P. (Eds.), European Neogene Mammal Chronology. Plenum Press, New York and London, pp. 73–90.

Negendank, J.F.W., Irion, G., Linden, J., 1982. Ein eozänes Maar bei Eckfeld nordöstlich Manderscheid (SW-Eifel, Bundesrepublik Deutschland). Mainzer Geowissenschaftliche Mitteilungen 11, 157–172.

Pérez-Obiol, R., Jalut, G., Julià, R., Pèlachs, A., Iriarte, M.J., Otto, T., Hernández-Beloqui, B., 2011. Mid-Holocene vegetation and climatic history of the Iberian Peninsula. The Holocene 21, 75–93.

Pirrung, M., Fischer, C., Büchel, G., Gaupp, R., Lutz, H., Neuffer, F.-O., 2003. Lithofacies succession of maar crater deposits in the Eifel area (Germany). Terra Nova 15, 125–132.

Popescu, S.-M., 2001. Repetitive changes in Early Pliocene vegetation revealed by high-resolution pollen analysis: revised cyclostratigraphy of southwestern Romania. Review of Palaeobotany and Palynology 120 (3–4), 181–202.

Popescu, S.M., Biltekin, D., Winter, H., Suc, J.-P., Melinte-Dobrinescu, M.C., Klotz, S., Rabineau, M., Combourieu-Nebout, N., Clauzon, G., Deaconu, F., 2010. Pliocene and Lower Pleistocene vegetation and climate changes at the European scale: long pollen records and climatostratigraphy. Quaternary International 219, 152–167.

Porreca, M., Mattei, M., Di Vincenzo, G., 2009. Postdeformational growth of late diagenetic greigite in lacustrine sediments from southern Italy. Geophysical Research Letters 36, L09307.

Riera, S., Esteban, A., 1994. Vegetation history and human activity during the last 6000 years on the central Catalan coast (northeastern Iberian Peninsula). Vegetation History and Archaeobotany 3, 7–23.

Roberts, A.P., Chang, L., Rowan, C.J., Horng, C.S., Florindo, F., 2011. Magnetic properties of sedimentary greigite ($Fe_3S_4$): an update. Reviews of Geophysics 49, RG1002.

Robinson, M.M., Dowsett, H.J., Chandler, M.A., 2008. Pliocene role in assessing future climate impacts. Eos 89, 500–502.

Rossignol-Strick, M., 1983. African monsoons, an immediate climate response to orbital insolation. Nature 304, 46–49.

Sagnotti, L., Roberts, A.P., Weaver, R., Verosub, K.L., Florindo, F., Pike, C.R., Clayton, T., Wilson, G.S., 2005. Apparent magnetic polarity reversals due to remagnetization resulting from late diagenetic growth of greigite from siderite. Geophysical Journal International 160, 89–100.

Sánchez Goñi, M.F., Landais, A., Fletcher, W.J., Naughton, F., Desprat, S., Duprat, J., 2008. Contrasting impacts of Dansgaard–Oeschger events over a western European latitudinal transect modulated by orbital parameters. Quaternary Science Reviews 27, 1136–1151.

Steininger, F.F., Berggren, W.A., Kent, D.V., Bernor, R.L., Sen, S., Agustí, J., 1996. Circum-Mediterranean Neogene (Miocene and Pliocene) marine–continental chronologic correlations of European mammal units. In: Bernor, R.L., Fahlbusch, V., Mittmann, H.W. (Eds.), The evolution of Western Eurasian Neogene Mammal Faunas. Columbia University Press, New York, pp. 7–46.

Suc, J.-P., 1984. Origin and evolution of the Mediterranean vegetation and climate in Europe. Nature 307, 429–432.

Suc, J.-P., Cravatte, J., 1982. Etude palynologique du Pliocène de Catalogne (nord-est de l'Espagne): apports à la connaissance de l'histoire climatique de la Méditerranée occidentale et implications chronostratigraphiques. Paléobiologie Continentale 13 (1), 1–31.

Suc, J.-P., Popescu, S.-M., 2005. Pollen records and climatic cycles in the Mediterranean region since 2.7 Ma. In: Head, M.J., Gibbard, P.L. (Eds.), Early–Middle Pleistocene Transitions, the Land–Ocean Evidence: Geological Society, London Special Publications, vol. 247, pp. 147–158.

Suc, J.-P., Diniz, F., Leroy, S., Poumot, C., Bertini, A., Dupont, L., Clet, M., Bessais, E., Zheng, Z., Fauquette, S., Ferrier, J., 1995. Zanclean (~Brunssumian) to early Piacenzian (~early–middle Reuverian) climate from 4° to 54° north latitude (West Africa, West Europe and West Mediterranean areas). Mededelingen Rijks Geologische Dienst 52, 43–56.

Suc, J.-P., Combourieu-Nebout, N., Seret, G., Klotz, S., Popescu, S.-M., Gautier, F., Clauzon, G., Westgate, J., Sandhu, A.S., 2010. The Crotone series: a synthesis and new data. Quaternary International 219, 121–133.

Tuenter, E., Weber, S.L., Hilgen, F.J., Lourens, L.J., 2003. The response of the African summer monsoon to remote and local forcing due to precession and obliquity. Global and Planetary Change 36, 219–235.

Tzedakis, P.C., 2007. Seven ambiguities in the Mediterranean palaeoenvironmental narrative. Quaternary Science Reviews 26, 2042–2066.

Tzedakis, P.C., Bennett, K.D., 1995. Interglacial vegetation succession: a view from southern Europe. Quaternary Science Reviews 14, 967–982.

Vehí, M., 2001. Geologia Ambiental de la Depressió de la Selva. PhD. Departament de Geologia Universitat Autònoma de Barcelona, Bellaterra (274 pp.).

Vehí, M., Pujadas, A., Roqué, C., Pallí, L., 1999. Un edifici volcànic inèdit a Caldes de Malavella (la Selva, Girona): El volcà del Camp dels Ninots. Quaderns de la Selva 1, 45–67.

Wang, C.W., 1961. The forests of China with a survey of grassland and desert vegetation. Maria Moors Cabot Fundation, vol. 5. Harvard University, Cambridge, Massachusetts.

Watts, W.A., 1985. A long pollen record from Laghi di Monticchio, southern Italy: a preliminary account. Journal of the Geological Society 142, 491–499.

Weaver, R., Verosub, K.L., Florindo, F., Pike, C.R., Clayton, T., Wilson, G.S., 2005. Apparent magnetic polarity reversals due to remagnetization resulting from late diagenetic growth of greigite from siderite. Geophysical Journal International 160, 89–100.

Whitlock, C., Anderson, R.S., 2003. Fire history reconstructions based on sediment records from lakes and wetlands. In: Veblen, T.T., Baker, W.L., Montenegro, G., Swetnam, T.W. (Eds.), Fire and Climatic Change in Temperate Ecosystems of the Americas, vol. 160. Springer-Verlag, New York, pp. 3–31.

Willis, K.J., Kleczkowski, A., Briggs, K.M., Gilligan, C.A., 1999. The role of sub-Milankovitch climatic forcing in the initiation of the Northern Hemisphere glaciation. Science 285, 568–571.

Zachos, J.C., Pagani, M., Sloan, L., Thomas, E., Billups, K., 2001. Trends, rhythms, and aberrations in global climate 65 Ma to present. Science 292, 686–693.